International Journal of Research and Development in Engineering Sciences
ISSN: 2582 - 4201(Online) , http://www.ijrdes.com/
Regular Issue, Vol. 8, Issue. 2 (March – April) , 2026 , Pages: 30 - 35
Received: 21 June 2025 ; *Accepted:* 28 March 2026 ; *Published:* 01 April 2026
https://doi.org/10.63328/IJRDES-V8RI2P5
Original Paper : Applied Research – Experimental Research Paper

Double Band E-Shaped Slotted Microstrip Hexagonal Patch Antenna

U Himaja Sree [1*] , Siva Suresh Kumar Gandi [2] , Sujatha Mandala [3] , R Ramana Reddy [4]

[1] UG Student, Dept. of ECE, JNTUA College of Engineering, Kalikiri, AP, India ; *uppuhimajasree@gmail.com*
[2] Asst. Professor, Dept. of ECE, Vignan's Institute of Engineering for women (A), Vishakhapatnam, AP, India; *suresh.ece@view.edu.in*
[3] Asst. Professor, Dept. of ECE, Lendi Institute of Engineering and Technology (A), Vizianagaram, AP, India; *sujatha.m@lendi.edu.in*
[4] Professor, Dept. of ECE, JNTUA College of Engineering, Kalikiri, AP, India, 517234; *profrrreddy@yahoo.co.in*

** Corresponding Author: U Himaja Sree ; uppuhimajasree@gmail.com*

Abstract: The design and analysis of a dual-band hexagonal microstrip patch antenna loaded with an E-shaped slot and a Hexagonal Defected Ground Structure (DGS) is proposed. The antenna is realized on a low-cost FR-4 epoxy substrate with a dielectric constant of 4.4 and a thickness of 1.6 mm. The radiating element comprises a hexagonal patch featuring modified edges and a central E-shaped slot. To implement the DGS, a hexagonal slot with a circumradius of 12.75 mm is introduced in the ground plane. Simulation results obtained using Ansys HFSS validate the antenna's operation at resonant frequencies of 4.025 GHz and 6.65 GHz, with bandwidths of 0.883 GHz (3.52–4.41 GHz) and 0.519 GHz (6.44–6.94 GHz), respectively. The proposed antenna reaches a maximum gain of 5.04 dBi at 6.65 GHz. Hence, the design is applicable to the current requirements of wireless communication.

Keywords: Hexagonal Microstrip Patch Antenna, E-Shaped Slot, DGS, and Dual-Band.

1. Introduction

The major factor for the widespread use of microstrip patch antennas in modern wireless networks is their low profile and cost-effective manufacturing techniques. However, patch antennas have some drawbacks, such as poor gain and bandwidth. In order to avoid these drawbacks, several investigations have been carried out on geometrical shapes such as hexagonal shapes and DGS.

Wideband and multi-band applications are effectively covered by hexagonal shapes. To illustrate this, a hexagonal slotted 5G energy harvesting antenna performed well at resonant frequencies of 4.6 GHz, 5.9 GHz, and 7.5 GHz with a stable radiation pattern [1]. Similarly, a hybrid dielectric resonator antenna consisting of a hexagonal ring patch antenna in combination with a ground slot has made it possible to achieve operation over seven different frequency bands, thus improving impedance bandwidth for 5G communications [2]. Hexagonal geometries have also been adapted for biomedical applications, where compact, low-profile multi-band designs are implemented to meet specific telemetry requirements [3]. The use of specific slot shapes in combination with DGS is of significant importance for improving gain levels and for operating in millimeter wave frequency ranges. A Pi-slotted microstrip patch antenna with a shaped DGS on a Rogers RT6002 substrate has been reported for achieving a maximum gain of 5.81 dBi at 41 GHz and 6.55 dBi at 73 GHz for 5G technology [4]. For the 5G band n78, a T-slotted antenna design working at a frequency of 3.5 GHz made use of a partial ground with a slot to achieve a return loss of -27.5 dB [5]. Further advancements include a DGS Antenna Array with interlinked Complementary Split Ring Resonators (CSRRs) operating in the 25–30 GHz band, which provides a high radiation gain of 7.75 dBi with a small footprint of 32 × 32 mm^2 [6]. Researchers have also studied the multi-band and wideband performance using parasitic elements and slots. A rectangular slotted antenna with parasitic elements exhibited multi-resonance performance over three frequency bands (2.35–2.47 GHz, 4.04–5.21 GHz, and 5.54–6.17 GHz), with the maximum gain being 4.54 dBi [7]. In order to obtain wideband circular polarization, an L-shaped patch placed in the rectangular slotted structure on the FR4 substrate resonated at 6.8 GHz with a gain of 9.7

ISSN: 2582 - 4201(Online) , http://www.ijrdes.com/ , IJRDES, Vol. 8, Issue 2 , 2026 , https://doi.org/10.63328/IJRDES-V8RI2P5

dB and an impedance bandwidth of 1300 MHz [8]. Furthermore, the optimization of fractal geometries such as a slotted koch snowflake patch resulted in a return loss of -26.8 dB at 2.07 GHz, thus making it effective for urban RF energy harvesting [9].

2. Related Research Work

Miniaturization and flexibility are two significant requirements in wearable and implantable devices. A compact implantable antenna enabled by DGS technology, designed on a Rogers 6010 substrate with a volume of merely 33.35 mm^3, has been shown to operate effectively in the 2.46 GHz ISM band [10]. For wearable telemetry, a semi-flexible slotted patch antenna working at 2.42 GHz frequency showed a fractional bandwidth of 1300 MHz with negligible performance degradation even when bent [11]. Likewise, a slotted antenna for a 2.45 GHz wearable application with symmetrical circular and U-slots resulted in a return loss of -38.45 dB, which validated the suitability of the antenna for WBAN application [12].

Despite extensive research on the hexagonal shape in previous studies, the design of a simple and high-gain dual-band antenna remains a problem. The existing design may not have a high gain and may not filter out the unwanted bands. Therefore, in order to overcome these problems, an E-shaped slot and a customized hexagonal defected ground structure are considered for the design of the antenna. The ground structure is designed in such a way that it will eliminate the third resonance. Therefore, the antenna will operate only in dual bands and will have a high return loss and a gain of 5.04 dBi. The design is made on a low-cost substrate of FR-4 epoxy material so that it is simple and compact [13]. The antenna is able to operate efficiently in two bands of 4.025 GHz and 6.65 GHz and is a very practical design for modern wireless communication systems. In this paper, a dual-band hexagonal patch antenna is proposed by introducing an E-shaped slot and a Hexagonal DGS. The antenna is designed to have resonance at two different frequencies and high gain [14]. The design process is explained step by step to understand the influence of the slot on the results. The important parameters of the design are also analyzed.

3. *Antenna Modeling*

In the proposed design, the antenna is a hexagonal patch with semicircular slots, which is combined with an E-shaped slot and DGS. The design is carried out on an FR4 epoxy dielectric substrate with a relative permittivity of 4.4 and thickness of 1.6 mm. Geometrical evolution is carried out in stages to achieve the desired wideband characteristics [16].

3.1. Hexagonal Patch Antenna (HPA)

The design process of the antenna is initiated by a basic form of a hexagonal patch antenna [17]. The antenna is constructed by a circular shape divided into six equal parts. The substrate of the microstrip patch antenna is made of FR-4 epoxy material of size 32x32 mm2 and a thickness of 1.6 mm. The radiating patch is a hexagon of side length (s) of 10 mm. The feed line dimensions are 6.3 mm(Lf) × 1 mm(Wf).The optimized antenna operates at three resonant frequencies, which are 4.375 GHz, 7.10 GHz, and 8.35 GHz. The return losses are -13.23 dB, -12.28 dB, and -11.49 dB, respectively. The bandwidths are 0.134 GHz (4.30–4.44 GHz), 0.171 GHz (7.01–7.18 GHz), and 0.197 GHz (8.26–8.46 GHz), respectively. The peak gain is 4.90 dBi, which is obtained at the resonant frequency of 4.375 GHz. Fig. 1 depicts the HPA, and Fig. 2 represents the return loss of the HPA.

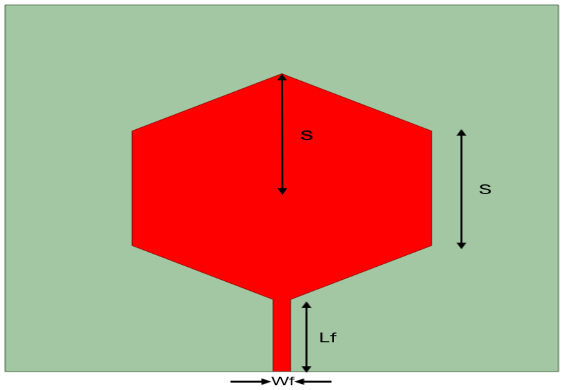

Figure. 1 Hexagonal Patch Antenna (HPA)

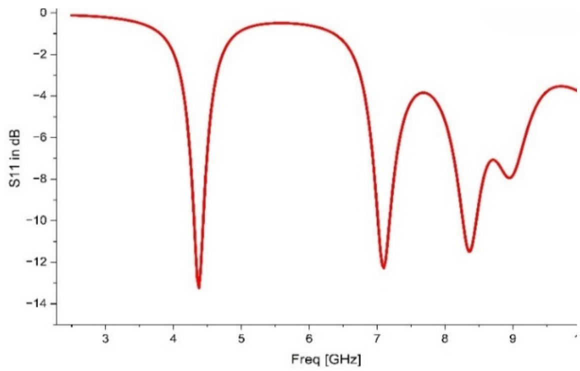

Figure. 2 Return loss of HPA

3.2. HPA with Semicircular Slots (HPA-SS)

This design is further refined by placing semicircular slots

Radius of slot (mm)	Resonant Frequency (GHz)	Band width (GHz)	Gain (dBi)
0.25	4.375, 7.125, 8.375	0.138, 0.164, 0.161	4.81, 2.32, 4.05
0.5	4.375, 7.075, 8.375	0.133, 0.152, 0.201	4.9, 2.19, 3.8
1	4.35, 7.0, 8.425	0.119, 0.082, 0.290	4.7, 1.99, 3.5

ISSN: 2582 - 4201(Online) , http://www.ijrdes.com/ , IJRDES, Vol. 8, Issue 2 , 2026 , https://doi.org/10.63328/IJRDES-V8RI2P5

along the edges of the hexagonal patch to enhance the antenna performance. Six semicircular slots of 0.5 mm in radius (Rs) are placed along the edges of the hexagon [18].

Table . 1 Parametric Study of the Semicircular Slot Radius (Rs)

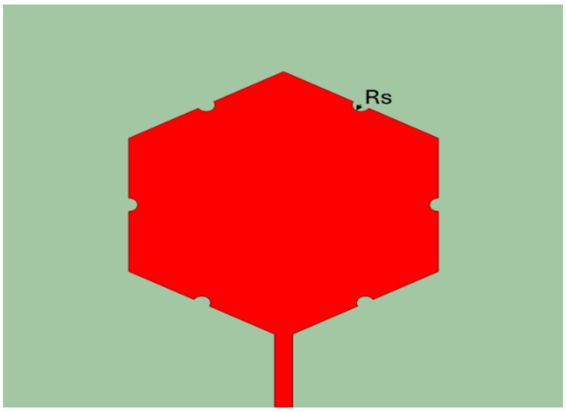

Figure. 3 HPA with Semicircular slots

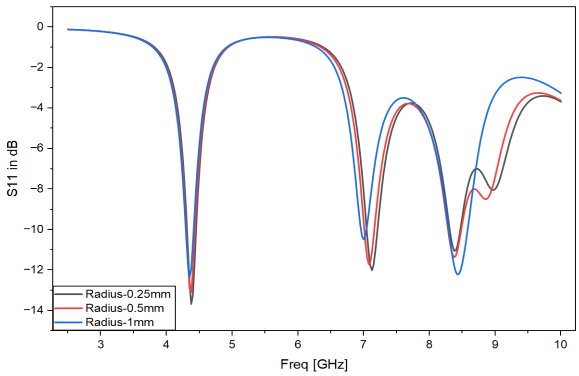

Figure. 4 Return loss of HPA-SS

A parametric analysis is carried out to achieve the optimal Rs by varying the dimensions of Rs to 0.25 mm, 0.5 mm, and 1 mm, as depicted in Fig. 4. The analysis reveals that an Rs of 0.25 mm yields bandwidths of 0.138 GHz (4.31–4.49 GHz), 0.164 GHz (7.04–7.20 GHz), and 0.161 GHz (8.30–8.46 GHz), with gains of 4.81 dBi at 4.375 GHz, 2.32 dBi at 7.125 GHz, and 4.05 dBi at 8.375 GHz.

Increasing Rs to 0.5 mm results in bandwidths of 0.133 GHz (4.29–4.43 GHz), 0.152 GHz (7.00–7.16 GHz), and 0.201 GHz (8.28–8.43 GHz) with gains of 4.9 dBi at 4.375 GHz, 2.19 dBi at 7.075 GHz, and 3.8 dBi at 8.375 GHz. Further increasing Rs to 1 mm results in bandwidths of 0.119 GHz (4.29–4.41 GHz), 0.082 GHz (6.95–7.03 GHz), and 0.29 GHz (8.28–8.57 GHz) with gains of 4.7 dBi at 4.35 GHz, 1.99 dBi at 7.0 GHz, and 3.5 dBi at 8.425 GHz.

Consequently, Rs = 0.5 mm was selected as the optimal dimension for the proposed antenna design. Comparing this to the fundamental HPA, the introduction of semicircular slots causes a slight frequency shift and bandwidth adjustment while maintaining triple-band performance. Fig. 3 illustrates the geometry of the HPA-SS, and Fig. 4 presents its return Loss (S11) parameters.

3.3. Hexagonal Patch Antenna with Semicircle and E-Shaped Slots (HPA-SES)

In the third stage of the design, an E-shaped slot is introduced in the radiating patch of the HPA-SS. The E-shaped slot is constructed using four rectangular cuts with the following dimensions: the vertical spine measures 4×0.5 mm^2, the top, middle, and bottom horizontal arms each measure 0.5×1.5 mm^2.

The dimensions of E-Slot are as follows:

a-b	**b-c**	**c-d**	**d-e**	**e-f**	**f-g**
4 mm	2 mm	0.5 mm	1.5mm	1.25mm	1.5 mm
g-h	h-i	i-j	j-k	k-l	l-a
0.5 mm	1.5 mm	1.25 mm	1.5 mm	0.5 mm	2 mm

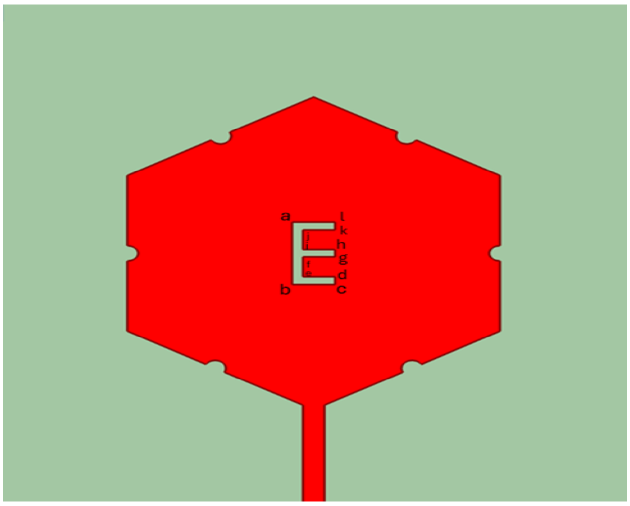

Figure. 5 HPA-SS with E-Shaped slot

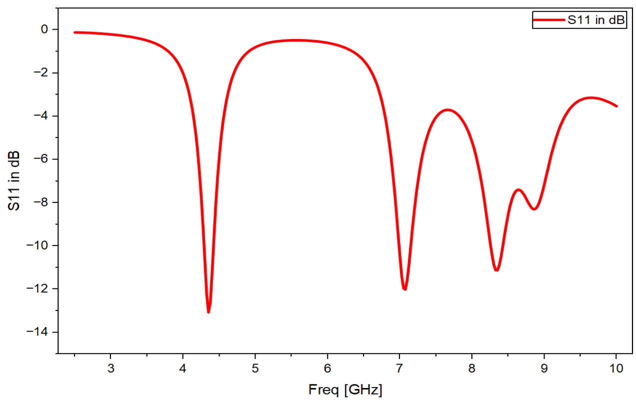

Figure. 6 Return loss of HPA-SES

The simulation results for the HPA-SES demonstrate effective triple-band operation following the introduction of the E-shaped slot. The antenna resonates at 4.35 GHz, 7.07 GHz, and 8.35 GHz. The return losses at these frequencies are -13.07 dB, -12.01 dB, and -11.12 dB, respectively. The design yields bandwidths of 0.130 GHz

ISSN: 2582 - 4201(Online) , http://www.ijrdes.com/ , IJRDES, Vol. 8, Issue 2 , 2026 , https://doi.org/10.63328/IJRDES-V8RI2P5

(4.28–4.41 GHz), 0.161 GHz (6.98–7.14 GHz), and 0.168 GHz (8.25–8.42 GHz). The gains observed at the three resonant frequencies are 4.89 dBi, 2.49 dBi, and 3.75 dBi. Fig. 5 illustrates the geometry of the HPA-E, and Fig. 6 presents its Return Loss (S11) parameters

3.4. Hexagonal Patch Antenna with E-Slot and DGS (Proposed Antenna)

In the final stage of the proposed design, a DGS is integrated in the ground plane of the HPA-SES to further enhance performance [20]. DGS is a technique where a specific shape is removed out of the metal ground layer to modify the antenna's characteristics [21][29]. In the proposed design, a hexagonal slot is centrally incorporated into the ground plane with a radius (Sd) of 12.75 mm. Three DGS configurations were investigated, as shown in Fig. 7.

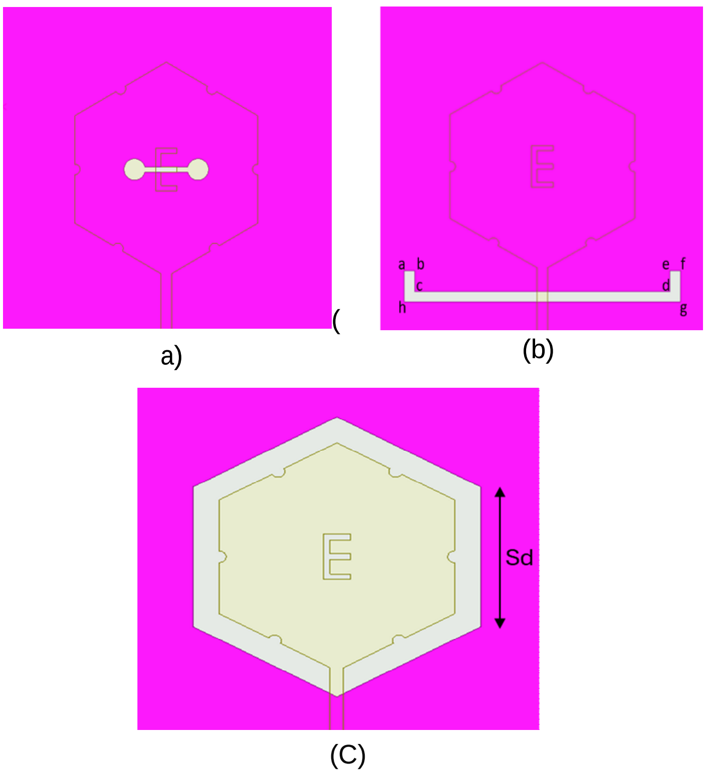

Figure. 7 E-shaped slotted HPA-SS with DGS (a) Circular dumbbell shaped DGS (b) U-shaped DGS (c) Hexagon shaped DGS

4. Results

The design of the suggested HPA-SES with various DGS configurations are presented in Fig. 7. To identify the optimal ground plane structure, three distinct DGS shapes were analyzed: (a) Circular dumbbell-shaped DGS, (b) U-shaped DGS, and (c) Hexagon-shaped DGS.

Fig. 8 presents the return loss (S11) parameters of the HPA-SES with these three different DGS configurations. The antenna with [22] the Circular dumbbell-shaped DGS exhibits operation at three frequency bands of 4.05 GHz, 7.05 GHz, and 8.4 GHz. The corresponding return losses are -13.79 at 4.05 GHz, -13.10 at 7.05 GHz, and -11.62 at 8.4 GHz [30][32]. The design results in bandwidths of 0.134 GHz (3.98–4.12 GHz), 0.185 GHz (6.97–7.15 GHz), and 0.255 GHz (8.28–8.53 GHz) with gains of 5.0 dBi at 4.05 GHz, 2.56 dBi at 7.05 GHz, and 3.09 dBi at 8.4 GHz.

The antenna with the U-shaped DGS operates at resonant frequencies of 3.8625 GHz, 7.0375 GHz, and 8.8125 GHz with corresponding return losses of -21.30, -14.42, and -13.70 respectively. The achieved bandwidths are 0.082 GHz (3.81–3.89 GHz), 0.242 GHz (6.92–7.17 GHz), and 0.227 GHz (8.68–8.91 GHz). The resulted gains at the respective resonant frequencies are 2.45 dBi, 3.76 dBi, and 2.88 dBi.

For the Hexagon-shaped DGS, a parametric study was conducted by varying the side length (Sd) of the hexagonal slot to tune the resonant frequencies and improve impedance matching [23]. The analysis confirmed that a side length of Sd = 12.75 mm yields the optimal dual-band characteristics [29] [31]. This finalized design operates over the frequency ranges of 4.025 GHz and 6.625 GHz with corresponding bandwidths of 0.883 GHz (3.52–4.41 GHz) and 0.519 GHz (6.44–6.94 GHz) respectively [24]. The maximum peak gain of 5.04 dBi is obtained at 6.625 GHz.

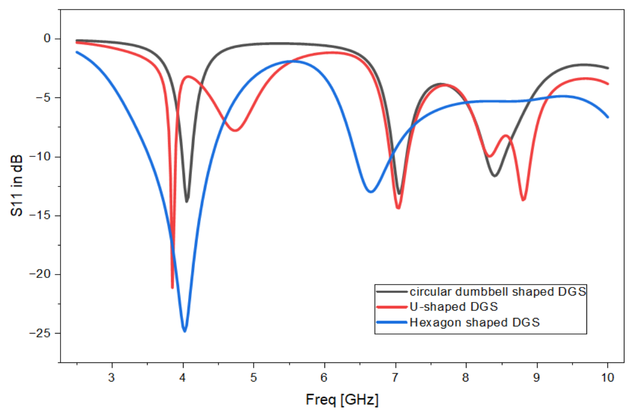

Figure. 8 Return loss of HPA with E-Slot and three different DGS configurations

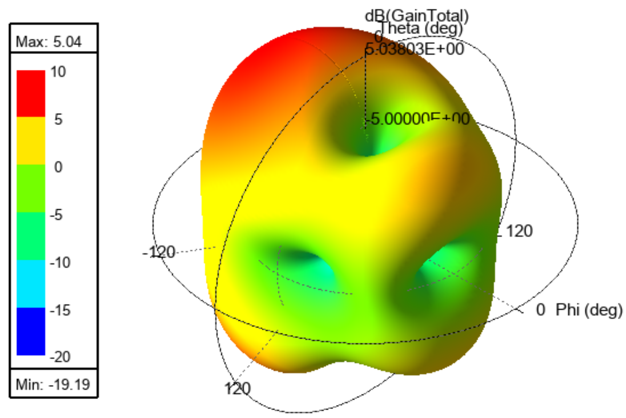

Figure. 9 Gain plot of Proposed HPA with E-Slot and DGS

ISSN: 2582 - 4201(Online) , http://www.ijrdes.com/ , IJRDES, Vol. 8, Issue 2 , 2026 , https://doi.org/10.63328/IJRDES-V8RI2P5

The dumbbell and U-shaped DGS maintained a weaker triple-band [25] [33], whereas the hexagon-shaped DGS removed the third resonance and resulted in a dual-band antenna. This dual-band configuration resulted in a much better return loss and gain, making [26] this configuration the best option. Based on the comparative performance analysis, the Circular dumbbell-shaped DGS and U-shaped DGS configurations exhibited triple-band characteristics [27] but with less significant return loss depths and lower gain values compared to the final design [28]. In contrast, the antenna employing the optimized Hexagon-shaped

Type of Antenna	Resonant Frequency (GHz)	Band width (GHz)	Gain (dBi)
Hexagonal patch	4.375, 7.1, 8.35	0.134, 0.171, 0.197	4.9, 2.4, 3.52
HPA with semicircle slots	4.375, 7.075, 8.375	0.133, 0.152, 0.201	4.9, 2.19, 3.8
HPA with E-shaped slot	4.35, 7.075, 8.35	0.130, 0.161, 0.168	4.89, 2.49, 3.75
Proposed antenna E-Shaped slotted HPA with DGS	4.025, 6.625	0.883, 0.519	4.61, 5.04

DGS demonstrated a dual-band response with superior return loss characteristics and enhanced gain performance [28] [34].

Table 2: Comparison among various stages of Antenna

Consequently, the Hexagon-shaped DGS with Sd = 12.75 mm was selected as the optimal configuration for the proposed design [29].

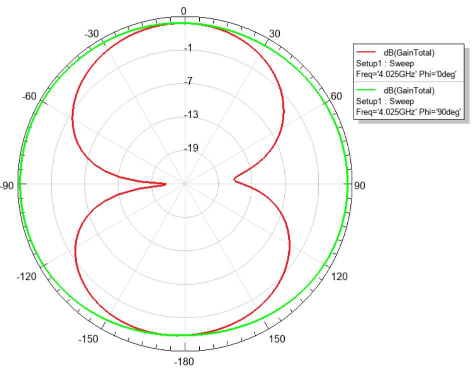

Fig. 10: E & H plane of Hexagonal Patch Antenna with E-Shaped slot and DGS at 4.025 GHz

The gain plot of the proposed antenna is shown in Fig. 9, while the E-plane and H-plane radiation patterns are presented in Fig. 10.

The proposed E-Shaped slotted antenna achieves multiband operation by providing two distinct bandwidths of 883 MHz and 519 MHz. Unlike the reference models that only operate on a single band, this design maintains a reasonable gains of 4.61 dBi and 5.04 dBi respectively. This demonstrates a superior balance between versatile frequency coverage and consistent signal strength compared to existing single-band models.

Table 3: Comparison of Proposed antenna with related works

Reference	Band width (MHz)	Gain (dBi)
[5]	1300	9.7
[6]	1300	2.5
Proposed antenna (E-Shaped slotted HPA with DGS)	883, 519	4.61, 5.04

5. Conclusion and Future Scope

A Hexagonal microstrip patch antenna with an E-Shaped slot and DGS is presented in this paper. With bandwidths of 0.883 GHz (3.52–4.41 GHz) and 0.519 GHz (6.44–6.94 GHz), the suggested antenna operates at the frequencies of 4.025 GHz and 6.65 GHz. At 6.65 GHz, the suggested antenna's peak gain is 5.04 dBi. This is useful for dual-band applications. Future work will focus on fabricating the physical prototype and conducting Vector Network Analyzer (VNA) measurements to experimentally validate the simulated results, as well as obtaining circular polarization within the operating bandwidth.

References

[1]. D. Singh, N. Kashyap, and A. Thakur, "Design and optimization of a hexagonal-slotted wideband microstrip antenna for 5 G networks RF energy harvesting," Franklin Open, vol. 13, art. no. 100409, 2025. doi: 10.1016/j.fraope.2025.100409.

[2]. M. Manikandan, S. P. J. Christydas, R. Saravanakumar, and S. A. A. Rajasree, "Enhanced Performance of Hybrid Dielectric Resonator Antenna with Hexagonal Ring Patch and Ground Slot for Multiband Operation in 5G Wireless Communication," Tehnički vjesnik, vol. 32, no. 1, pp. 313–318, 2025. doi: 10.17559/TV-20240515000000.

[3]. S. Elangovan, R. Gokul Raj, and M. Maheswari, "Design and analyzing of hexagon-shaped microstrip patch antenna for biomedical applications," ResearchGate, Art. no. 371024845, Jun. 2023.

[4]. B. R. Dutta and B. M. Naikoo, "Design and Analysis of Advance DGS Pi-Slotted Microstrip Patch Antenna for 5G Applications," in Advanced Computing Techniques in Engineering and Technology, Singapore: Springer Nature, 2026, pp. 1–12. doi: 10.1007/978-981-97-7654-2_1.

[5]. M. Nesasudha, N. Moses, and D. K. Janapala, "A T-Slotted Compact Sized Antenna for 5G n78 Band Applications," International Journal of Wireless Information Networks, vol. 32, no. 1, pp. 45–58, 2025. doi: 10.1007/s10776-024-00642-x.

[6]. E. M. Ali, M. I. Khattak, W. Hussain, and T. A. Khan, "Defected ground structure antenna array with metasurface inspired interlinked CSRR for 5G millimeter wave applications," Scientific

ISSN: 2582 - 4201(Online) , http://www.ijrdes.com/ , IJRDES, Vol. 8, Issue 2 , 2026 , https://doi.org/10.63328/IJRDES-V8RI2P5

Reports, vol. 15, no. 1, art. no. 14185, 2025. doi: 10.1038/s41598-025-54321-x.

[7]. S. S. Khade, P. L. Zade, C. V. Bawankar, S. G. Kanade, and A. B. Nandgaonkar, "A Rectangular Slotted Microstrip Patch Antenna with Parasitic Elements," in *Lecture Notes in Networks and Systems*, vol. 1358, Singapore: Springer Nature, 2026, pp. 309–321. doi: 10.1007/978-981-97-7543-9_25.

[8]. M. K. C. Durbhakula, S. Aouthu, and P. Bharghava, "Wide Band Circularly Polarized Slotted Microstrip Patch Antenna for Wireless Applications," in *EAI* International Conference on Advanced Technologies in Electronics, Communications and Signal Processing (ICETECSP), Singapore: Springer Nature, 2024, pp. 273–284. doi: 10.1007/978-3-031-70000-0_23.

[9]. M. W. Seng, H. L. Shareef, P. Y. Chan, M. K. A. Rahim, N. A. Murad, and G. A. E. Aziz, "Experimental investigation on slotted Koch snowflake fractal patch rectenna," *Scientific Reports*, vol. 15, no. 1, art. no. 34601, 2025. doi: 10.1038/s41598-025-82410-y.

[10]. S. B. Abdulkareem and K. Ramasamy, "DGS enabled compact implantable antenna with minimal SAR for biomedical applications," Frequenz, vol. 79, no. 1, pp. 45–58, 2025. doi: 10.1515/freq-2024-0125.

[11]. D. R. Varma, M. V. Subbarao, C. Grandhi, and S. S. D. Kameswari, "Design of Semi-flexible Slotted Patch Antenna for Biomedical Applications," in Advanced Technologies in Electronics, Communications and Signal Processing, Singapore: Springer Nature, 2025, pp. 285–294. doi: 10.1007/978-3-031-70000-0_24.

[12]. M. Dileep, N. Moses, and D. K. Janapala, "A Slotted Antenna for 2.45GHz Wearable Applications," in EAI International Conference on Advanced Technologies in Electronics, Communications and Signal Processing (ICETECSP), Singapore: Springer Nature, 2024, pp. 261–272. doi: 10.1007/978-3-031-70000-0_22.

[13]. S. V. M. K and S. A, “Traffic Sign Detection and Recognition using Deep Learning,” International Journal of Research and Development in Engineering Sciences, vol. 6, no. 1, p. 22, Jan. 2024, doi: 10.63328/ijrdes-v6ri1p5.

[14]. A. K. D, “CIVIC EYE: AI - Powered Public Safety Assistant,” International Journal of Computational Science and Engineering Research, vol. 3, no. 1, p. 86, Jan. 2026, doi: 10.63328/ijcser-v3ri1p10.

[15]. K. Venkata, D. M, V. Ch, and S. R. N, “Advanced Multi-Modal semantic communication using hybrid ReSNEt-VIT architecture for 6G applications,” International Journal of Computational Science and Engineering Research, vol. 3, no. 1, p. 74, Jan. 2026, doi: 10.63328/ijcser-v3ri1p9.

[16]. G. P. S and S. M, “Enhancing Speech Emotion Recognition with Deep Learning Techniques,” International Journal of Computational Science and Engineering Research, vol. 3, no. 1, p. 1, Jan. 2026, doi: 10.63328/ijcser-v3ri1p1.

[17]. R. N, “The impact of digital transformation on leadership and management styles,” International Journal of Computational Science and Engineering Research, vol. 2, no. 1, Mar. 2025, doi: 10.63328/ijcser-v2ri1p6.

[18]. S. K. N and S. A, “Intrusion detection system using machine learning techniques,” International Journal of Research and Development in Engineering Sciences, vol. 6, no. 2, p. 4, Apr. 2024, doi: 10.63328/ijrdes-v6ri2p2.

[19]. N. R. Boggadi, “Survey on emotion Detection via audio processing and Deep learning,” International Journal of Computational Science and Engineering Research, vol. 2, no. 2, p. 30, Jun. 2025, doi: 10.63328/ijcser-v2ri2p6.

[20]. D. Bhuvannagari and S. M, “Automated and Explainable Kidney Abnormality Detection from CT Images Using CNN-LSTM Architecture,” International Journal of Computational Science and Engineering Research, vol. 2, no. 3, p. 1, Jul. 2025, doi: 10.63328/ijcser-v2i3p1.

[21]. S. Dekka and N. R. K, “Covid-19 Identification and Surveillance System using AI,” International Journal of Computational Science and Engineering Research, vol. 2, no. 1, p. 5, Oct. 2024, doi: 10.63328/ijcser-v1ri1p2.

[22]. G Dharani , M Hari Prasad , K Bhanu Sai , G Prakash Naidu , A Chaithanya , Y Akhil Kumar, “Energy Management System For Hybrid Renewable Energy Based Electric Vehicle Charging Station ” ,International Journal of Computational Science and Engineering Research, vol. 1, no. 2, May. 2024, doi: https://doi.org/10.63328/IJCSER-V1RI2P7

[23]. P. Tarollu and B. R. Y, “Intelligent Chatbot ticketing system using RNN and CNN,” International Journal of Research and Development in Engineering Sciences, vol. 7, no. 1, p. 30, Feb. 2025, doi: 10.63328/ijrdes-v7ri1p6.

[24]. A. Raju, A. Augustine, C. E. S. S, and S. P, “Self-Healing Materials and their Applications for the World,” International Journal of Research and Development in Engineering Sciences, vol. 5, no. 6, p. 1, Nov. 2023, doi: 10.63328/ijrdes-v5ri6p1.

[25]. K. Venkata, D. M, V. Ch, and S. R. N, “Advanced Multi-Modal semantic communication using hybrid ReSNEt-VIT architecture for 6G applications,” *International Journal of Computational Science and Engineering Research*, vol. 3, no. 1, p. 74, Jan. 2026, doi: 10.63328/ijcser-v3ri1p9.

[26]. M. S. S, A. R. T, V. P, and N. Gandla, “An Attention-Enhanced YOLOV8 model for accurate Multi-Class kidney abnormality detection in CT imaging,” *International Journal of Computational Science and Engineering Research*, vol. 3, no. 1, p. 68, Jan. 2026, doi: 10.63328/ijcser-v3ri1p8.

[27]. A. K. D, “CIVIC EYE: AI - Powered Public Safety Assistant,” *International Journal of Computational Science and Engineering Research*, vol. 3, no. 1, p. 86, Jan. 2026, doi: 10.63328/ijcser-v3ri1p10.

[28]. S. R. Ramireddy and V. S. K. A, “A hybrid framework combining preprocessing, VGG-19 transfer learning, and GPT enhanced CLIP for Fine-Grained Classification,” *International Journal of Computational Science and Engineering Research*, vol. 3, no. 1, p. 60, Jan. 2026, doi: 10.63328/ijcser-v3ri1p7.

[29]. S. P. K. Gudla, P. Nutipalli, and C. R. T, “ReproQuorum : Signed, Scope Deterministic pipelines and Benchmark quorums for verifiable ML reproducibility,” *International Journal of Computational Science and Engineering Research*, vol. 3, no. 1, p. 52, Jan. 2026, doi: 10.63328/ijcser-v3ri1p6.

[30]. K. R. Kuppireddy, R. T, R. Yagireddi, and J. V. G. P. R. Pyla, “Real-Time Stampede Risk Prediction from Crowd Videos Using YOLOv8 and Spatio-Temporal Modeling,” *International Journal of Computational Science and Engineering Research*, vol. 3, no. 1, p. 44, Jan. 2026, doi: 10.63328/ijcser-v3ri1p5.

[31]. S. Kodeboina, A. Sk, and M. M. T, “Spatio-Temporal modeling for abnormal behaviour detection in crowd scenes,” *International Journal of Computational Science and Engineering Research*, vol. 3, no. 1, p. 37, Jan. 2026, doi: 10.63328/ijcser-v3ri1p4.

[32]. P. Ch, V. N. C. K. Pulipati, and V. Kalla, “Leveraging ChatGLM-LORA for Scalable Mental Health interventions: a Cognitive Behavioural Therapy,” *International Journal of Computational Science and Engineering Research*, vol. 3, no. 1, p. 15, Jan. 2026, doi: 10.63328/ijcser-v3ri1p3.

[33]. R. T and K. R. Kuppireddy, “A multimodal deep learning framework for robust person Re-Identification,” *International Journal of Computational Science and Engineering Research*, vol. 3, no. 1, Jan. 2026, doi: 10.63328/ijcser-v3ri1p2.

[34]. G. P. S and S. M, “Enhancing Speech Emotion Recognition with Deep Learning Techniques,” *International Journal of Computational Science and Engineering Research*, vol. 3, no. 1, p. 1, Jan. 2026, doi: 10.63328/ijcser-v3ri1p1.

Declaration

Conflicts of Interest: The authors declare no conflict of interest.

Author Contribution: All authors wrote the main manuscript text and also consent to the submission.

Ethical approval: Not applicable.

Consent to Participate: All authors consent to participate.

Funding: Not applicable, and No funding was received

Institutional Review Board Statement: Not applicable.

Informed Consent Statement: Not applicable.

Personal Statement: We declare with our best of knowledge that this research work is purely Original Work and No third party material used in this article drafting. If any such kind material found in further online publication, we are responsible only for any judicial and copyright issues.

Acknowledgements

We thank everyone who inspired our work.